

# Parallel solid synthesis of inhibitors of the essential cell division FtsZ enzyme as a new potential class of antibacterials

Catherine Paradis-Bleau,<sup>a</sup> Mélanie Beaumont,<sup>b</sup> François Sanschagrin,<sup>a</sup>  
Normand Voyer<sup>b</sup> and Roger C. Levesque<sup>a,\*</sup>

<sup>a</sup>CREFSIP, Département de Biologie Médicale, Faculté de médecine, Université Laval, Sainte-Foy, Que., Canada G1K 7P4

<sup>b</sup>CREFSIP, Département de chimie, Faculté des sciences et génie, Université Laval, Sainte-Foy, Que., Canada G1K 7P4

Received 10 July 2006; revised 2 November 2006; accepted 8 November 2006

Available online 10 November 2006

**Abstract**—As a model system for designing new inhibitors of bacterial cell division, we studied the essential and highly conserved FtsZ GTPase from *Pseudomonas aeruginosa*. A collection of GTP analogues were prepared using the solid-phase parallel synthesis approach. The synthesized GTP analogues inhibited the GTPase activity of FtsZ with IC<sub>50</sub> values between 450 μM and 2.6 mM, and 5 compounds inhibited *Staphylococcus aureus* growth in a biological assay. The FtsZ spectrophotometric assay developed for screening of synthesized compounds is the first step in identification of antibacterials targeting the bacterial cell division essential proteins. © 2006 Elsevier Ltd. All rights reserved.

## 1. Introduction

The widespread misuse of antibiotics has applied an immense pressure selecting for bacteria resistant to all classes of antibiotics. The critical human health outcome of antibiotic resistance among bacterial pathogens worldwide necessitates the development of structurally new antibacterials against targets essential for growth, whose inhibition should give a lethal phenotype.<sup>1</sup> The bacterial cell division process encodes essential proteins forming the divisome representing some of the best antibacterial targets. These proteins are extremely sensitive to inhibition since the cell division depends on recruitment of specific proteins in an essential cascade for forming the divisome.<sup>2,3</sup> Among those proteins, we selected FtsZ as a specific target because this is the most important and conserved protein of the cell division machinery.<sup>4</sup> FtsZ is at the top of hierarchic recruitment in the divisome and its polymerization into the Z-ring allows the physical separation of daughter cells.<sup>5</sup> The polymerization of FtsZ depends upon GTP hydrolysis and this essential enzymatic activity can be exploited to screen inhibitory molecules.<sup>6</sup> The FtsZ strategy proposed here is supported by the absence of bacterial resistance against FtsZ

inhibitors MinC and SulA which constitute active regulators of cell division.<sup>7,8</sup> We focused efforts on the FtsZ protein of *Pseudomonas aeruginosa*, one of the major opportunistic pathogens causing severe nosocomial infections.<sup>9,10</sup> We used FtsZ from *P. aeruginosa* because this bacterium is extensively studied as a model system resistant to most antibiotics. FtsZ is highly conserved amongst bacteria and we also tested compounds for growth inhibition of *Staphylococcus aureus* because of the differences in permeability between both species and because of the MRSA problem.

To develop drugs with novel structures, we decided to synthesize a manageable number of molecules by combinatorial chemistry. This technology allows the quick generation of large numbers of structurally related compounds.<sup>11</sup> Combinatorial chemistry was first developed to synthesize peptides but we adapted recent advances to small organic compound synthesis.<sup>12</sup> This approach can be achieved either in solution or in solid-phase. We opted for the time-saving solid support strategy permitting to obtain higher yields where automated reactions can be accelerated by using excess reagents, simplified washing and purification steps.<sup>12</sup> We thus used the solid-phase chemistry method to synthesize GTP analogues and parallel synthesis was adopted to branch out rapidly the core structure to obtain sufficient amounts of unique small organic compounds in the library.

**Keywords:** Parallel synthesis; GTP analogues; *Pseudomonas aeruginosa* FtsZ inhibitors; *Staphylococcus aureus*.

\* Corresponding author. Tel.: +1 418 656 3070; fax: +1 418 656 7176; e-mail: [rclevesq@rsvs.ulaval.ca](mailto:rclevesq@rsvs.ulaval.ca)

This work identifies a new potential class of antibacterial agents targeting the essential FtsZ cell division GTPase. We describe the synthesis of highly diversified GTP analogues having chosen unique structures as potential FtsZ inhibitors. The GTP binding and hydrolytic activities of the purified *P. aeruginosa* FtsZ protein were characterized. The inhibitory activity of each synthesized GTP analogue was then evaluated individually in vitro against the FtsZ GTPase activity and in vivo on whole bacterial cells. As part of our continued interest in the development of novel antimicrobials using essential targets, we present here the development of a simple, cost-effective, and rapid assay for screening FtsZ GTPase inhibitors.

## 2. Results

### 2.1. Purification of the *P. aeruginosa* FtsZ protein

The FtsZ protein was efficiently expressed in soluble form in the cytoplasmic fraction of *Escherichia coli* BL21 ( $\lambda$ DE3) cells as depicted in Figure 1, lane 1. The nickel affinity chromatography permitted the purification of FtsZ with a yield of 20 mg/L. The purified FtsZ protein was visualized as a single 42 kDa band on SDS-PAGE (Fig. 1, lane 2). N-terminal sequencing of the first 15 amino acid residues confirmed the identity of the purified protein as *P. aeruginosa* FtsZ (100% identity with the published sequence).

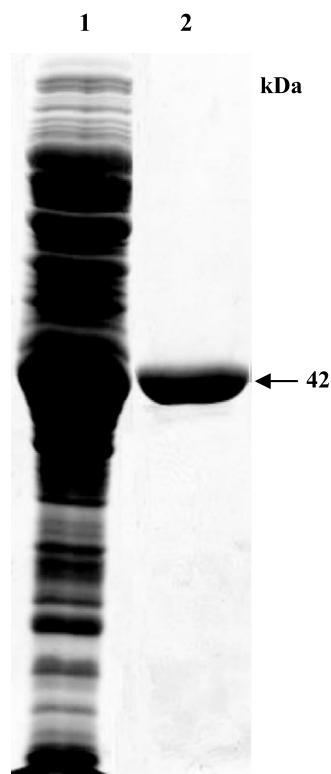


**Figure 1.** SDS-PAGE showing overexpression of the FtsZ protein in *E. coli* BL21 ( $\lambda$ DE3) cells (Lane 1) and the near homogeneity of the purified FtsZ protein (Lane 2).

### 2.2. Characterization of the GTP binding and GTPase hydrolysis activity of purified FtsZ

An UV cross-link binding assay was performed to characterize the substrate specificity of FtsZ. The autoradiography showed that FtsZ binds preferentially GTP amongst the four radioactive nucleotides tested as substrates (Fig. 2A). The negative control included in the GTPase assay described in Section 4.3 gave no GTP hydrolysis (Fig. 2B). This assay showed that the purified FtsZ was biologically active when using 12  $\mu$ M FtsZ which hydrolyzed 85% of the  $P^{32}$ -labeled GTP substrate into GDP after 1 h at 37 °C (Fig. 2B).

### 2.3. Strategy, design, and synthesis of GTP analogues in the library

A combination of solid-phase combinatorial chemistry and parallel synthesis was used to synthesize highly diversified GTP analogues. The general strategy was optimized from published procedures to allow a  $S_N2$  nucleophilic attack of 2-amino-6-chloropurine on the  $\beta$ -lactone 2.<sup>13,14</sup> The  $\beta$ -lactone opening was done by a nucleophilic attack on the  $sp^3$  carbon at the  $\beta$  position of the cycle and not on the  $sp^2$  carbon. The hydroxyl function of the serine was thus substituted by the 2-amino-6-chloropurine by a nucleophilic attack of the  $N^9$  atom of the purine. The central nucleus of molecules was a guanine moiety linked to an Ala called GAL core structure (Figs. 3 and 4). To obtain the desired library, an *N*-tert-butoxycarbonyl (Boc)-protected guanine modified amino acid (product 4 in Fig. 3) was required. The *N*-(Boc)-(2-amino-6-chloropuryl)-L-Ala (4) was synthesized by the formation of a  $\beta$ -lactone and its opening by 2-amino-6-chloropurine (3). The most critical step was the formation of the Ser  $\beta$ -lactone (product 2 in Fig. 3) from the (Boc)-L-Ser. This step was achieved by the Mitsunobu reaction with variable and modest yields between 25% and 40%. Different methods were attempted to improve yield of this critical step. The method described by Slidregta gave similar yields but involved a trityl protecting group.<sup>15</sup> The use of dimethylazodicarboxylate or diisopropylazodicarboxylate instead of diethylazodicarboxylate (DEAD) gave lower yields and the method based upon the mixed anhydrides was not successful (data not shown).<sup>16</sup> We thus optimized the Mitsunobu reaction and the yield was raised to 87.7% of a 99% pure product when working on a small scale. Analysis of the purified Ser  $\beta$ -lactone product by NMR spectroscopy confirmed the structure (see Section 4). We observed that the purification process must be done as rapidly as possible to avoid a re-opening of the  $\beta$ -lactone cycle. The guanine group was then added on the side chain of Ser  $\beta$ -lactone by a nucleophilic displacement reaction using 2-amino-6-chloropurine giving 4 (see Section 4).

The core structure 4 was utilized for parallel synthesis and the oxime resin was chosen as solid support. This resin displayed an oxime function linked on a polystyrene bead permitting the cleavage with different nucleophiles to obtain more functional diversity. The initial amino acid was linked on the resin by the formation

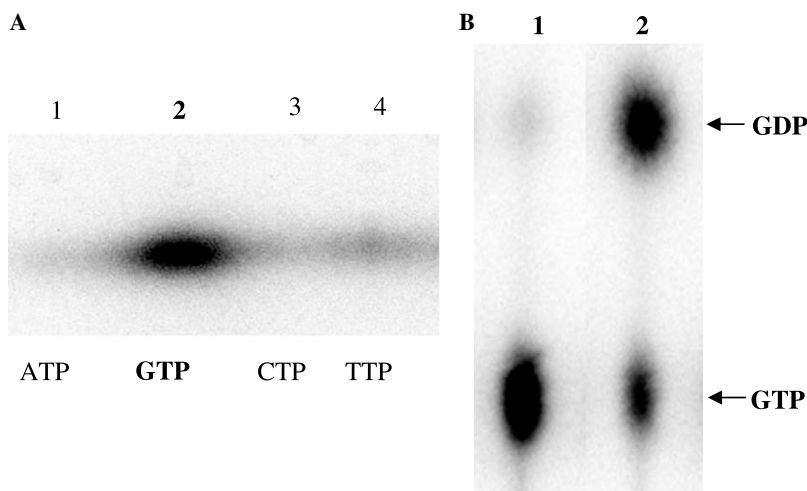


**Figure 2.** (A) UV cross-link specific nucleotide binding assay showing that FtsZ binds preferentially GTP. (B) Autoradiogram demonstrating FtsZ GTPase activity. Lanes: 1, control without enzyme; 2, hydrolysis of GTP to GDP by FtsZ.

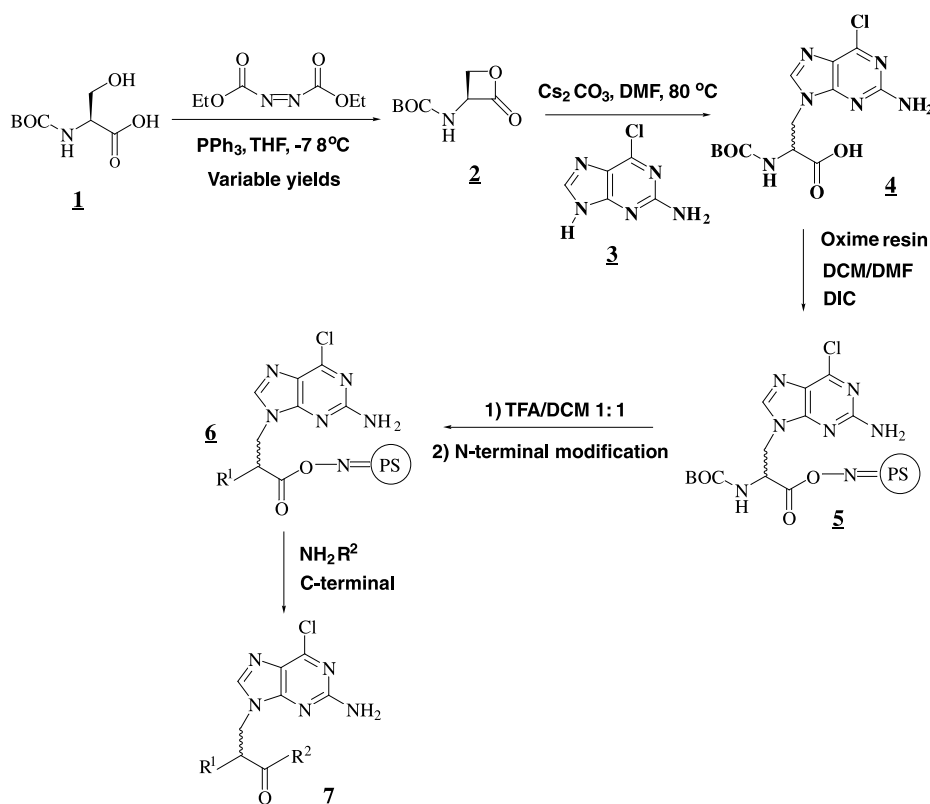


**Figure 3.** Solid-support combinatorial chemistry strategy and chemical reactions used to synthesize the library of GTP analogues.

of an ester bond between the carboxylic acid of the amino acid and the oxime resin. This bond was sufficiently stable under anhydrous acidic conditions to use a BOC protection strategy and to permit the N-terminal modification of the core structure. After transformations, the C-terminal was modified by cleavage of the bound ester with nucleophiles using relatively mild conditions. The target compounds illustrated in Figure 4 were synthesized via modification of both N- and C-terminals of the core structure. Six different chemical  $\text{R}^1$  groups were used to modify the functionality of the N-

terminal and three different  $\text{R}^2$  nucleophiles were used to adapt the C-terminal (Fig. 4). We thus synthesized nine different low molecular weight molecules.

LC/MS and  $^1\text{H}$  NMR analyses confirmed the expected structure of each compound (see Section 4). In mass spectrometry, molecular ion  $(\text{M}+\text{H})^+$  peak was observed for **12** and **14**, whereas the  $\text{M}^+$  peak was observed for other compounds. All observed  $m/z$  data corresponded to the exact calculated mass of the compounds. The mass spectrometry results also confirmed that chloropurine

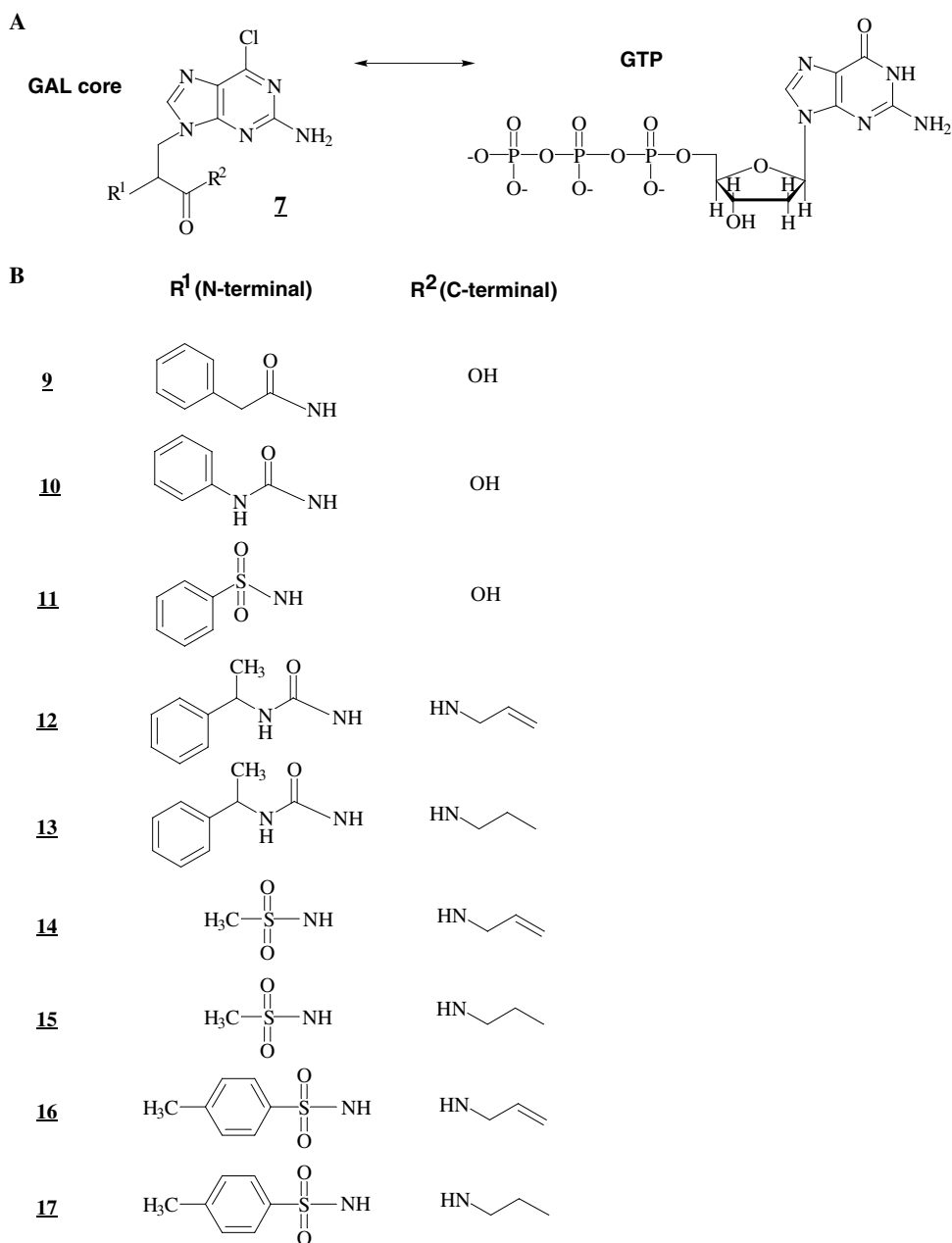


**Figure 4.** (A) GAL core mimicking the natural GTP substrate of FtsZ; the relative positions of side chains R<sup>1</sup> and R<sup>2</sup> used for the parallel synthesis are indicated. (B) Chemical structure of individual GTP analogues found in the library with R<sup>1</sup> and R<sup>2</sup> groups used to modify the N- and C-terminal of the GAL core.

was not hydrolyzed to a guanine function during acid treatment required for BOC deprotection. All spectroscopic data confirmed the chemical structures of compounds described in Figure 4.

#### 2.4. Development of a screening assay for FtsZ inhibitors

We developed a rapid and reliable screening assay to evaluate the GTPase FtsZ inhibitory potential of synthesized molecules. A spectrophotometric coupled enzymatic assay was used which allowed quantitative analysis of the FtsZ GTPase activity with high sensibility and rapidity. We decided to determine initial velocities for all GAL compounds and results for compounds

**10**, **14**, and **15** are presented in Table 1. Quantitative analysis of the FtsZ GTPase enzymatic reaction was done by monitoring the oxidation of NADH as a decrease in absorbance at 340 nm described in Section 4.5 and in Figure 5.

#### 2.5. Evaluation of GTP analogues as inhibitors of the GTPase activity of FtsZ

Synthesized compounds were analyzed for their capability to inhibit GTPase activity of FtsZ in vitro. The FtsZ conversion of GTP into GDP was used to assess the inhibitory properties of the synthesized compounds. All the GTP analogues inhibited the GTPase activity

**Table 1.** Initial velocities of three synthesized compounds used to calculate IC<sub>50</sub> values

Compound <sup>a</sup>	Concentration (mM)	V <sub>0</sub> (ΔDO <sub>340 nm</sub> /min)
<b>10</b>	0	0.014
	0.3	0.010
	0.5	0.007
	0.7	0.004
	0.9	0.003
	1.3	0
<b>14</b>	0	0.014
	0.3	0.013
	0.5	0.012
	0.6	0.007
	0.7	0.004
	0.9	0
	1.3	0
<b>15</b>	0	0.014
	0.3	0.013
	0.5	0.011
	0.7	0.007
	0.8	0.006
	0.9	0.005
	1.1	0.004
	1.2	0

<sup>a</sup> Initial velocities were determined with FtsZ for each of the nine compounds using a spectrophotometric coupled enzyme assay with NADH (Fig. 5). Details are given in Section 4.5.

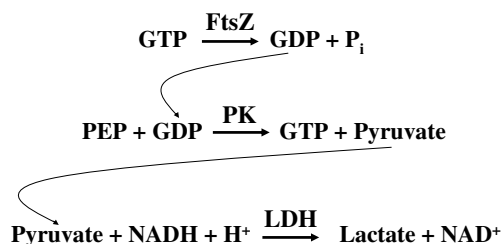


**Figure 5.** Spectrophotometric FtsZ enzymatic coupled assay. The GDP product of FtsZ is used as substrate with phosphoenol pyruvate (PEP) by the pyruvate kinase (PK) enzyme that gave GTP and pyruvic acid. The pyruvic acid is used as substrate with NADH + H<sup>+</sup> by the lactate dehydrogenase (LDH) enzyme giving lactate and NAD<sup>+</sup>. The NADH + H<sup>+</sup> molecule can be detected at 340 nm but the final NAD<sup>+</sup> product gave no absorbance at 340 nm.

of FtsZ with significant IC<sub>50</sub> values between 450 μM and 2.6 mM as given in Table 2. Each compound showed a linear response between an increase in concentration and a decrease of the GTPase activity. This correlation is well represented by compound **14** in Figure 6. The inhibition curves of all nine inhibitors displayed a sigmoidal dose–response trend having variable slopes as shown in Figure 6. GTP analogues included in control reactions did not affect the PK and LDH enzyme reaction rate (see Section 4.6 and in Fig. 5) used to measure the release of GDP by FtsZ. The nine GTP analogues thus specifically inhibited FtsZ.

## 2.6. Testing of synthesized compounds in a biological assay

The antibacterial activity of GTP analogues was evaluated with *E. coli* and *S. aureus* cells. Kanamycin used

**Table 2.** IC<sub>50</sub> values and antibacterial activity for the nine FtsZ inhibitors synthesized<sup>a</sup>

Compound	MW (g/mol)	IC <sub>50</sub> (mM)	Antibacterial <sup>b</sup> (mm)
<b>9</b>	356	2	No inhibition
<b>10</b>	357	0.45	10
<b>11</b>	378	1.2	No inhibition
<b>12</b>	424	1.8	No inhibition
<b>13</b>	426	1.8	11
<b>14</b>	355	0.6	28
<b>15</b>	357	0.7	15
<b>16</b>	431	1.7	No inhibition
<b>17</b>	433	2.6	11

<sup>a</sup> Molecular weight (MW) are indicated along with the IC<sub>50</sub> value for each GTP analogue inhibiting the GTPase activity of FtsZ. The activity was measured by a coupled enzyme spectrophotometric assay.

<sup>b</sup> Antibacterial activity of the GAL compounds was evaluated by a biological assay using *S. aureus* cells and the measurement of the diameter of the zone of inhibition of growth.

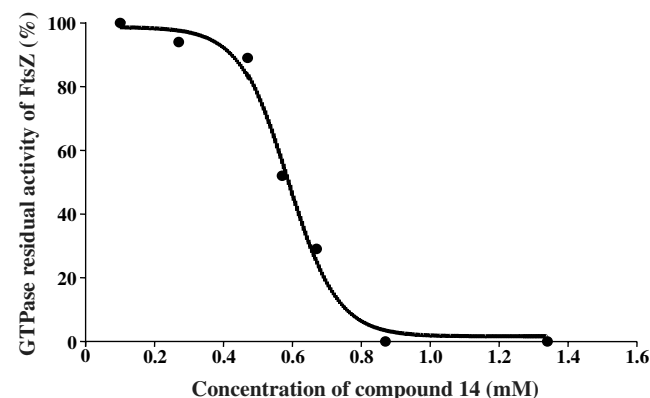


**Figure 6.** IC<sub>50</sub> determination for the compound **14** inhibitor of the GTPase activity of FtsZ. The residual activity of FtsZ was measured as a function of the concentration of **14**. The positive control used with GDP showed a rapid decrease in absorbance at 340 nm indicating that the coupled enzymatic assay was efficient. The negative control performed without the FtsZ enzyme gave a stable absorbance at 340 nm in a time-dependent fashion. This demonstrated that the drop of absorbance in the FtsZ assay was attributable to the FtsZ GTPase activity.

as a control showed an inhibition of growth with a diameter of 30 mm at 20 g/L for both species (Fig. 7). None of the GAL compounds inhibited *E. coli* growth. Among the nine synthesized compounds, **5** inhibited *S. aureus* growth (Fig. 7 and Table 2). Compounds **14** and **15** showed the most promising antibacterial activity with inhibition of growth having a diameter of 28 and 15 mm, respectively, at 20 g/L. Compounds **10**, **13**, and **17** presented a moderate antibacterial activity at 20 g/L (Fig. 7 and Table 2).

## 3. Discussion

In the last few years, there has been growing interest in identifying new antibacterial targets using essential proteins implicated in cell growth and division.<sup>17</sup> Until recently, bacterial cell division proteins such as FtsZ



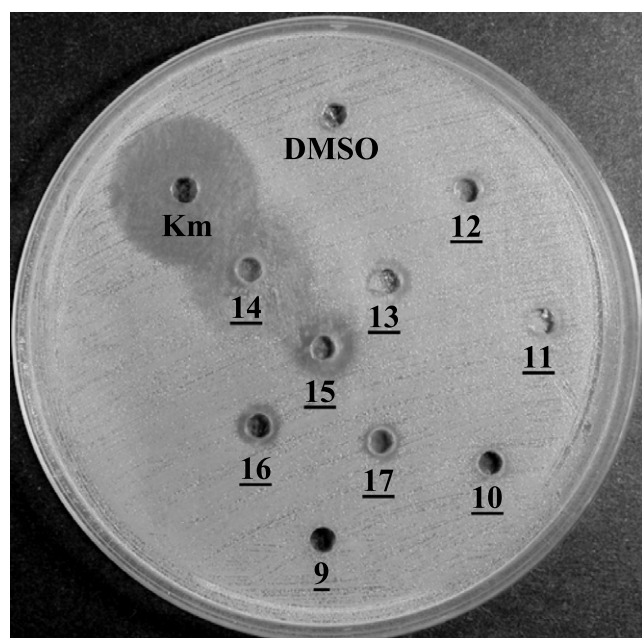


**Figure 7.** Agar diffusion assay showing inhibition of growth of *S. aureus* by GAL compounds.

had not been used as targets and no pharmacologically active inhibitors of division proteins identified. We targeted the most conserved and essential cell division protein FtsZ which polymerizes as a ring to allow septation of daughter cells via an essential GTPase activity.<sup>4,6</sup> The GTPase activity of FtsZ was confirmed.<sup>7</sup> It has previously been shown that FtsZ binds GTP.<sup>18</sup> Here, we demonstrated the strong binding affinity and specificity of FtsZ for the GTP substrate.

Since FtsZ specifically binds and hydrolyzes GTP via an essential activity, we developed active inhibitors mimicking the natural GTP substrate.<sup>6,19</sup> To optimize the specificity of inhibitors for FtsZ and restrict their interference in eukaryotic cells, we have synthesized a core structure composed of a guanine-like moiety linked to an Ala side chain. We argued that the guanyl group will form a bond in the FtsZ active site. Synthesized compounds will thus either compete with the natural substrate as competitive inhibitors or block the GTP binding to FtsZ by restricting access to the active site and act as irreversible inhibitors.

The core structure was quite tedious to obtain on a large scale. We optimized the method described by Pansare and we used the more reactive 2-amino-6-chloropurine instead of a guanine surpassing the yield of other methods.<sup>20–22,15,16</sup> Concerning the preparation of the  $\beta$ -lactone, the optimized Mitsunobu reaction allowed the synthesis of **2** in good yields only when working on a small scale; whereas it was previously reported as 72% in yield when starting from 5 g of (Boc)-L-Ser.<sup>13,14</sup> Several attempts for preparing the  $\beta$ -lactone and using 5 g of (Boc)-L-Ser as described previously gave poor yields which could be due to variations in the quality of (Boc)-L-Ser preparations used.

The diversity of compounds in our focus library was created by substituting the core structure at the N- and C-terminal positions. The oxime resin was used as the most convenient solid support for our parallel synthesis strategy in comparison to other support such as the Merrifield resin.<sup>12,23,24</sup> This strategy is most efficient in Boc, permits gentle cleavage with nucleophiles, and eventually permits incorporation of a C-terminal amino group in a single step. A vast majority of the chemical groups in R<sup>1</sup> used to modify the N-terminal functionality were aromatics as many known antibiotics possess an aromatic group. We also minimized the bulk of the R<sup>2</sup> group so as to presumably facilitate the binding in the FtsZ GTP active site.

Various methods have already been used to evaluate the biological activity of FtsZ. The FtsZ GTPase activity was quantified via hydrolysis of radioactive GTP substrate.<sup>6,25</sup> The FtsZ activity was also quantified by measuring the release of inorganic phosphate or by assessing protein polymerization.<sup>26–28</sup> These methods required high amounts of FtsZ except for radioactive assays. The spectrophotometric assay permitted to follow in real time the GTPase reaction in comparison to other assays where only end-point data are obtained. Our assay is also less time-consuming, cost-effective, highly reproducible, and could be well adapted to a HTS screening in microtiter plates.

The GAL core structure of analogues was efficient in mimicking GTP and impairing the FtsZ activity. First, we determined their initial velocity (Table 1) and used these data to calculate IC<sub>50</sub> values which were in the  $\mu$ M range (Table 2). The most active compounds were **10**, **14**, and **15**. The three best FtsZ inhibitors showed an antibacterial activity against *S. aureus*. Compound **14** is the most promising structure giving the best antibacterial activity and an IC<sub>50</sub> value of 600  $\mu$ M. As shown in Figure 4, the sole difference between compounds **14** and **15** is the presence of a double bond at the C-terminus of **14**. We will focus efforts to pursue characterization of **14** and its chemical structure will constitute the basic core structure for synthesis of more potent FtsZ inhibitors.<sup>29–31</sup>

FtsZ shares a highly conserved central core structure with tubulin.<sup>32,33</sup> However, FtsZ has a N-terminal extension absent in tubulin, while tubulin subunits display two long C-terminal  $\alpha$ -helices absent in FtsZ.<sup>34</sup> Several tubulin inhibitors are presently used in cancer treatment, but are not very effective against FtsZ.<sup>35,36</sup>

To date, few FtsZ inhibitors have been identified.<sup>25,37–42</sup> The Zantrin compounds perturb the FtsZ ring assembly causing lethality to a variety of bacteria in broth cultures, indicating that FtsZ antagonists may serve as chemical leads for the development of new broad-spectrum antibacterial agents.<sup>43</sup> The antibacterial activity of GAL compounds may be similar to Zantrins and could be attributable to inhibition of the Z-ring polymerization dependent on the FtsZ GTPase activity.<sup>43</sup> The viriditoxin product from *Aspergillus* sp. MF6890 blocked FtsZ polymerization with an IC<sub>50</sub> of

8.2  $\mu\text{g/mL}$  and inhibited GTPase activity with an  $\text{IC}_{50}$  of 7.0  $\mu\text{g/mL}$ .<sup>41</sup> The antibacterial action of viriditoxin via inhibition of FtsZ was confirmed by the observation of its effects on cell morphology, macromolecular synthesis, DNA-damage response, and increased minimum inhibitory concentration as a result of an increase in FtsZ expression. Viriditoxin exhibited broad-spectrum antibacterial activity against clinically relevant Gram-positive pathogens, including methicillin-resistant *S. aureus* and vancomycin-resistant *Enterococci*, without affecting the viability of eukaryotic cells.<sup>41</sup> The sole GTP analogue identified as an FtsZ inhibitor did not have antibacterial activity.<sup>44</sup> The 8-bromoguanosine 5'-triphosphate acts as a competitive inhibitor of both FtsZ polymerization and GTPase activity with a  $K_i$  of 31.8  $\mu\text{M}$ . The observation that this GTP analogue did not inhibit tubulin assembly suggested a structural difference of the GTP-binding pockets of FtsZ and tubulin.<sup>44</sup> Structures of the published FtsZ inhibitors could be exploited to enhance the inhibitory potential of compound **14**.<sup>40,43</sup>

To our knowledge, this is the first report describing GTP analogues having promising inhibitory properties of the GTPase activity of FtsZ and validated antimicrobial properties against whole bacterial cells. The synthesis of derivatives of these compounds is a promising avenue in investigating the structure–activity relationships for the design of efficient and specific inhibitors of bacterial cell division and we are currently working along these lines.

## 4. Experimental

### 4.1. Reagents, solvents, and bacterial strains

Amino acids were purchased from Advanced ChemTech (Louisville, Kentucky, USA) and all other reagents were purchased from Sigma–Aldrich (Oakville, Ontario, Canada) unless otherwise indicated. The reagents and solvents were treated as follows: dichloromethane (DCM) was distilled; dimethylformamide (DMF) was degassed using nitrogen; water was deionized and filtered using a 0.45  $\mu\text{m}$  membrane; tetrahydrofuran (THF) was distilled over Na and benzophenone; *n*-propylamine was distilled over KOH. Other reagents and solvents were used directly; methanol ACS grade (EM Science, VWR International, Mont-Royal, Québec, Canada); acetonitrile spectroscopic quality (Laboratoire MAT, Beauport, Québec, Canada); diethyl ether ACS grade (BDH, VWR International); chloroform spectroscopic quality. The recombinant plasmid containing the *ftsZ* gene was propagated in *E. coli* NovaBlue, *endA1 hsdR17 r<sub>K12</sub><sup>-</sup> m<sub>K12</sub><sup>+</sup> supE44 thi-1 recA1 gyrA96 relA1 lac [F' proA<sup>+</sup>B<sup>+</sup> lacI<sup>q</sup>  $\Delta$  M15::Tn10]* prior to protein synthesis in *E. coli* BL21, *F<sup>-</sup> ompT hsdS<sub>B</sub> r<sub>B</sub><sup>-</sup> m<sub>B</sub><sup>-</sup> gal dcm* ( $\lambda$ DE3) (Novagen, Madison, WI, USA).

### 4.2. Purification of biologically active FtsZ enzyme

Polymerase chain reaction (PCR) amplification was used to obtain DNA fragments encoding *P. aeruginosa*

PAO1 *ftsZ* gene. The construction fused a His-tag at the C-terminus of the FtsZ protein. The *ftsZ* PCR product was cloned into the expression vector pET24b (Novagen) as described previously.<sup>45</sup> The recombinant plasmid pMON2020 containing the *ftsZ* gene was maintained in *E. coli* NovaBlue prior to protein expression in *E. coli* BL21.<sup>45</sup> Expression of the recombinant FtsZ protein was performed by adding 1 mM IPTG at an OD 600 nm of 0.8 during the exponential phase of growth. The *E. coli* BL21 culture was then incubated for 4 h at 37 °C under agitation. Cells were centrifuged and the bacterial pellet was treated with lysozyme and sonicated.<sup>45</sup> FtsZ was purified to homogeneity by affinity chromatography using a His-bind nickel resin (Novagen) with 150 mM imidazole during elution. Purified FtsZ was dialyzed in buffer (20 mM Tris–HCl, pH 7.6, 10 mM NaCl, and 1 mM EDTA) and conserved in 50% (v/v) glycerol at –80 °C.<sup>46</sup> Purified FtsZ was visualized on SDS–PAGE and the protein concentration was determined using the Bradford method (Bio-Rad, Mississauga, Ontario, Canada). N-terminal sequencing was done by the Edman degradation technique at the Biotechnology Research Institute (National Research of Council Canada, Montreal, Québec, Canada).<sup>45</sup>

### 4.3. Biochemical characterization of FtsZ

An UV cross-link specific nucleotide-binding assay was performed with purified FtsZ and with the radioactive nucleotides ATP, GTP, CTP, and TTP.<sup>47</sup> Briefly, 3  $\mu\text{g}$  of purified FtsZ was mixed with each of the four  $\text{P}^{32}$ -labeled nucleotides (Perkin-Elmer, Woodbridge, Ontario, Canada). The samples were incubated for 30 min at 0 °C and irradiated for 10 min at 254 nm in a microtiter plate on top of a chilled lead brick in iced water. The samples were purified prior to analysis by SDS–PAGE and visualized by autoradiography. The GTPase activity of purified FtsZ was confirmed using a thin-layer chromatography (TLC) assay with  $\text{P}^{32}$ -labeled GTP as substrate. The FtsZ GTPase assay was performed using 12  $\mu\text{M}$  FtsZ in reaction buffer Z (50 mM Bis-Tris propane, pH 7.4, 10 mM  $\text{MgCl}_2$  and 2.5 mM DTT) and 1  $\mu\text{L}$  of  $\text{GTP}^{32}$  10  $\mu\text{Ci}/\mu\text{L}$  (Perkin-Elmer) in a final volume of 20  $\mu\text{L}$ .<sup>25</sup> The mixture was incubated for 1 h at 37 °C and 2  $\mu\text{L}$  was deposited on a TLC along with a negative control (without enzyme). Hydrolysis of the radioactive substrate was measured by autoradiography using a Phosphorimager (Fuji, Stanford, California, USA).

### 4.4. Synthesis of the GTP analogue library using combinatorial chemistry

**4.4.1. Synthesis of the  $\beta$ -lactone **2** from (Boc)-L-Ser.** The general strategy was from Pansare et al.<sup>21</sup> The method was optimized on a small scale and the reaction was repeated to accumulate the desired amount of (Boc)-L-Ser  $\beta$ -lactone **2**. In a typical experiment (1 g, 4.87 mmol) (Boc)-L-Ser (1 g, 4.87 mmol) was dissolved in 5 mL of anhydrous THF and the solution was introduced in an addition funnel on a 100 mL 3-necked flask. Triphenylphosphine (1.28 g, 4.87 mmol) was added to the reaction mix and the assembly was kept under inert atmosphere.

Twenty-five microliters of anhydrous THF was added to dissolve triphenylphosphine and the solution was cooled down to  $-78^{\circ}\text{C}$  using a dry ice-acetone bath. When the temperature was stable, DEAD (0.77 mL, 4.87 mmol) was added dropwise over a period of 10 min at constant temperature. The (Boc)-L-Ser solution was then added dropwise over a period of 15 min. After an agitation period of 20 min at  $-78^{\circ}\text{C}$ , the temperature was slowly raised to room temperature. The mixture was stirred for 2.5 h and the solvent was evaporated to precipitate the triphenylphosphine oxide. A column chromatography was performed to purify the (Boc)-L-Ser- $\beta$ -lactone product using silica gel as adsorbent and a hexane/AcOEt 65:35 at elution.

**4.4.2. Ser  $\beta$ -lactone (2).** HPLC:  $R_t = 10.9$  min.  $^1\text{H}$  NMR (300 MHz,  $\text{DMSO}-d_6$ )  $\delta$ : 1.41 (s, 9H, *t*-butyl), 4.29 and 4.41 (7 lines, 2H,  $J_{\text{AB}} = 4.5$  Hz,  $\text{CH}_2$ ), 5.14 (m, 1H,  $\text{CH}_\alpha$ ), 7.81 (d, 1H,  $\text{NH}$ , 8.0 Hz).  $^{13}\text{C}$  NMR (75 MHz,  $\text{DMSO}-d_6$ )  $\delta$ : 28.1 ( $\text{CH}_3$  *t*-butyl), 58.8 ( $\text{CH}_2$ ), 65.8 ( $\text{CH}_\alpha$ ), 79.3 (C *t*-butyl), 154.7 ( $\text{C}=\text{O}$  *t*-butyl), 170.6 ( $\text{C}=\text{O}$ ). Yield: 87.7%; purity >99%.

**4.4.3. Opening of the  $\beta$ -lactone 2 and formation of *N*-(Boc)-(2-amino-6-chloropuryl)-L-Ala (4).** (Boc)-L-Ser- $\beta$ -lactone (1.4 g, 7.5 mmol) and 2-amino-6-chloropurine (1.9 g, 11.2 mmol, 1.5 equiv) were dissolved in 20 mL of anhydrous DMF. Cesium carbonate (3.66 g, 11.2 mmol) was added and the solution was heated to reflux during 3 h. The solution was cooled and water was added to stop the reaction. The pH was adjusted to 5 and 6 extractions were done using 20 mL of ethyl acetate with moderate agitation. The organic phase was dried with anhydrous  $\text{MgSO}_4$ , filtered, evaporated, and kept under vacuum.

**4.4.4. *N*-(Boc)-(2-amino-6-chloropuryl)-L-Ala (4).** HPLC:  $R_t = 10.66$  min. MS (MALDI-TOF):  $m/z$  357.1 = ( $\text{M}+\text{H}$ ) $^+$ .  $^1\text{H}$  NMR (300 MHz,  $\text{DMSO}-d_6$ )  $\delta$ : 1.30 (s, 9H, *t*-butyl), 4.24 (m, 1H,  $\text{CH}_\alpha$ ), 4.44 (m, 2H,  $\text{CH}_2$ ), 6.97 (s, 2H,  $\text{NH}_2$ ), 7.31, (d, 1H,  $J = 8$  Hz  $\text{NH}$ ), 7.95, (s, 1H,  $\text{CH}=\text{N}$ ), 13.01 (m, 1H,  $\text{COOH}$ )  $^{13}\text{C}$  NMR (75 MHz,  $\text{DMSO}-d_6$ )  $\delta$ : 28.02 ( $\text{CH}_3$  *t*-butyl), 43.49 ( $\text{CH}_2$ ), 52.44 ( $\text{CH}_\alpha$ ), 78.59 (C *t*-butyl), 123.29 ( $\text{C1}-\text{C}=\text{N}$ ), 143.44 ( $\text{CH}=\text{N}$ ), 149.32 ( $\text{NH}_2-\text{C}=\text{N}$ ), 154.16 ( $\text{C}=\text{C}$ ), 155.26 ( $\text{C}=\text{C}$ ), 159.83 ( $\text{C}=\text{O}$  *t*-butyl), 171.24 ( $\text{COOH}$ ). Yield: 63.7%; purity >96%.

**4.4.5. Preparation of the oxime resin.** To obtain the desired oxime resin, polystyrene beads reticulated with divinylbenzene were treated with *p*-nitrobenzoyl chloride following the Friedel-Crafts conditions.<sup>23,24</sup> Once the acylation of the polystyrene was completed, hydroxylamine gave a reaction with the ketone to yield the oxime groups. After several washes, the oxime resin was composed of 1% divinylbenzene crosslinked polystyrene with randomly grafted *p*-nitrobenzoyloxime groups.

**4.4.6. Coupling of the GAL core molecule 4 on oxime resin.** Oxime resin (5 g) with a loading of 0.5 mmol/g was introduced into a solid-phase synthesis vessel with a sintered glass extremity and a Teflon cap. The resin was

swollen with 100 mL DCM and washed twice with 100 mL of this solvent. *N*-(Boc)-(2-amino-6-chloropuryl)-L-Ala **4** (3.66 g, 11.2 mmol) was dissolved in 80 mL of a DCM/DMF 1:1 mixture and the solution was cooled to  $0^{\circ}\text{C}$ . 1.26 mL of diisopropylcarbodiimide (DIC) (10.0 mmol; 4.0 equiv) was added and the suspension was shaken for 30 min. The resulting suspension was poured into the reaction vessel containing the oxime resin. The resulting mixture was shaken during 24 h, and its content was filtered by suction. The resin coupled with *N*-(Boc)-(2-amino-6-chloropuryl)-L-Ala was washed 3 times with 100 mL of DMF and 3 times with 100 mL of methanol. Washing steps were repeated and the resin was dried under vacuum.

**4.4.7. Acetylation of non-substituted sites on the oxime resin.** The non-substituted sites were blocked by acetylation as described in the literature.<sup>48</sup> Briefly, the resin was washed with DMF and an acetic anhydride/DMF 1:1 mixture was added to the vessel followed by DIEA. After 2 h of shaking, the content was filtered and the resin was washed with DMF, with methanol and then dried under vacuum. In this specific case, the concentration of resin to be loaded cannot be determined by the Kaser's quantitative colorimetric ninhydrin test because of the guanine moiety.<sup>49</sup> We pursued the synthesis assuming a substitution level of 0.4 mmol/g of dried resin.

**4.4.8. Deprotection of the *n*-Boc group of GAL core molecule.** Resin **5** was swollen with 100 mL DCM and washed twice with 100 mL of this solvent. Eighty microliters of a 2,2,2-trifluoroacetic/DCM 1:1 mixture was added and the mixture was shaken mechanically for 30 min. The vessel content was filtered by suction, washed with DMF and with methanol as mentioned above, and dried under vacuum.

**4.4.9. Modification of the N-terminal of GAL core molecule ( $\text{R}^1$ ).** The resin (500 mg, 0.20 mmol) was swollen with 10 mL DMF and washed twice with this solvent. An excess of 1 mmol (5 equiv) of the desired  $\text{R}^1$  group was added to the resin solution with 5 mL DCM and shaken for 2 h. The  $\text{R}^1$  group was obtained from carboxylic acids, acid chlorides, isocyanates or sulfonyl chlorides. In the case of the carboxylic acids, it was activated with DIC and hydroxybenzotriazole (HOBt). To do so, 1 mmol (5 equiv) of the carboxylic acid was dissolved in 8 mL of a DCM/DMF 1:1 mixture and the solution was cooled to  $0^{\circ}\text{C}$ . One hundred and fifty-seven microliters of DIC (1 mmol; 5 equiv) was added and the solution was shaken for 5 min. One hundred and thirty-five micrograms of HOBt- $\text{H}_2\text{O}$  (1 mmol and 5 equiv) was added and the whole mixture was shaken for 30 min. The suspension was introduced into the vessel, 52  $\mu\text{L}$  DIEA (0.3 mmol; 1.5 equiv) was added, and the content was shaken for 2 h. For each  $\text{R}^1$  group, the ampoule content was filtered by suction, washed with DMF and methanol as described previously, and dried under vacuum. For N-terminal modifications with acid chlorides, isocyanates or sulfonyl chlorides, the deprotected resin was swollen and washed with DMF. The acid solution of the desired reagent (5 equiv) in DCM was added to the resin, followed by addition of



52  $\mu$ L DIEA. After 2 h of shaking, the reaction mixtures were filtered, washed with a cycle of DMF and methanol, and then dried under vacuum to yield the appropriate N-modified compounds linked to the resin.

#### 4.4.10. Cleavage and modification of the C-terminal ( $R^2$ ).

The cleavages were performed using three nucleophiles: sodium hydroxide, *n*-propylamine or allylamine.<sup>50</sup> The sodium hydroxide cleavage was done by first swelling the resin with 20 mL THF and washing it twice with 20 mL of this solvent. Thirty microliters of a THF solution containing 10% of 0.1 N NaOH was introduced into the reaction vessel and the resulting mixture shaken for 4 h. The vessel content was filtered by suction and washed 3 times with 30 mL DCM and 30 mL of methanol. This step was repeated and the solvents and washings were combined and evaporated under vacuum. The dried crude product was dissolved in glacial acetic acid and lyophilized. The *n*-propylamine cleavage was done by treating the swollen resin in DCM with 20  $\mu$ L (1 equiv) of *n*-propylamine and 30 mL DCM. The resulting mixture was shaken for 1 h.<sup>50</sup> The vessel content was then recovered and the resin treated as described for the sodium hydroxide cleavage. The allylamine cleavages were performed as with *n*-propylamine.

#### 4.4.11. Synthesis of the specific compounds in library.

Each molecule under investigation was synthesized in a parallel fashion using the general method described previously.

**4.4.12. *N*-Phenylacetyl-(2-amino-6-chloropureryl)-L-Ala (9).** HPLC:  $R_t$  = 9.5 min. MS (API-ES):  $m/z$  373.2 =  $M^+$ .  $^1H$  NMR (300 MHz, DMSO- $d_6$ ): 3.65 (s, 2H,  $CH_2$ ), 4.37 (m, 1H,  $CH_\alpha$ ), 4.63 (d, 1H,  $J$  = 4.0 Hz,  $CH_2$  ala), 4.71 (d, 1H,  $J$  = 4.2 Hz,  $CH_2$  ala), 7.06–7.31 (m, 5H,  $H_{arom}$ ), 8.51 (s, 1H, N-CH=N). Yield: 61%; purity >95%.

**4.4.13. *N*-Phenylcarbamoyl-(2-amino-6-chloropureryl)-L-Ala (10).** HPLC:  $R_t$  = 5.4 min. MS (API-ES):  $m/z$  374 =  $M^+$ .  $^1H$  NMR (300 MHz, DMSO- $d_6$ ): 4.24 (m, 1H,  $CH_\alpha$ ), 4.51 (m, 2H,  $CH_2$  ala), 6.61 (d, 1H,  $J$  = 5.25 Hz,  $NH_\alpha$ ), 6.72 (s, 1H,  $NH-C_6H_5$ ), 7.16–7.49 (m, 5H,  $H_{arom}$ ), 8.08 (s, 1H, N-CH=N). Yield: 84%; purity >95%.

**4.4.14. *N*-Benzenesulfonyl-(2-amino-6-chloropureryl)-L-Ala (11).** HPLC:  $R_t$  = 10.3 min. MS (API-ES):  $m/z$  395 =  $M^+$ .  $^1H$  NMR (300 MHz, DMSO- $d_6$ ): 4.33 (m, 1H,  $CH_\alpha$ ), 4.52 (m, H,  $CH_2$ ), 6.86 (d, 1H,  $J$  = 10.6 Hz,  $NH$ ), 7.24–7.98 (m, 5H,  $H_{arom}$ ), 8.08 (s, 1H, N-CH=N). Yield 43%; purity >96%.

**4.4.15. Allyl amide of *N*-(*R*)-(+)- $\alpha$ -methylbenzylcarbamoyl-(2-amino-6-chloropureryl)-L-Ala (12).** HPLC:  $R_t$  = 13.7 min. MS (API-ES):  $m/z$  443 = ( $M+H$ ) $^+$ .  $^1H$  NMR (300 MHz, DMSO- $d_6$ ): 1.31 (m, 2H,  $CH_2=CH-CH_2$ ), 1.24 (d, 3H,  $J$  = 7.3 Hz,  $CH-CH_3$ ), 3.64 (m, 1H,  $CH-CH_3$ ), 5.05 (m, 1H,  $CH_\alpha$ ), 5.28 (m, 2H,  $CH_2$  ala), 5.82 (m, 2H,  $CH_2=CH-CH_2$ ), 5.94 (m, 1H,  $CH_2=CH-$

$CH_2$ ), 7.30 (m, 5H,  $H_{arom}$ ), 7.95 (s, 1H, N-CH=N). Yield 23%; purity >96%.

**4.4.16. *n*-Propyl amide of *N*-(*R*)-(+)- $\alpha$ -methylbenzylcarbamoyl-(2-amino-6-chloropureryl)-L-Ala (13).** HPLC:  $R_t$  = 15.1 min. MS (API-ES):  $m/z$  443 =  $M^+$ .  $^1H$  NMR (300 MHz, DMSO- $d_6$ ): 0.92 (t, 3H,  $J$  = 7.7 Hz,  $CH_3-CH_2-CH_2$ ), 1.39 (m, 2H,  $CH_3-CH_2-CH_2$ ), 2.05 (d, 3H,  $J$  = 7.5 Hz,  $CH_3-CH$ ), 2.75 (m, 2H,  $CH_3-CH_2-CH_2$ ), 2.98 (q, 1H,  $J$  = 6.1 Hz,  $CH_3-CH$ ), 3.65 (m, 2H,  $CH_2$  ala), 3.80 (m, 1H,  $CH_\alpha$ ), 7.34 (m, 5H,  $H_{arom}$ ). Yield: 24%; purity >96%.

**4.4.17. Allyl amide of *N*-methanesulfonyl-(2-amino-6-chloropureryl)-L-Ala (14).** HPLC:  $R_t$  = 4.7 min. MS (API-ES):  $m/z$  374 = ( $M+H$ ) $^+$ .  $^1H$  NMR (300 MHz, DMSO- $d_6$ ): 1.28 (m, 2H,  $CH_2-CH=CH_2$ ), 2.31 (s, 3H,  $CH_3$ ), 3.70 (m, 2H,  $CH_2$  ala), 5.02 (m, 1H,  $CH_\alpha$ ), 5.41 (d, 2H,  $CH_2=CH$ ), 5.89 (m, 1H,  $CH_2=CH$ ), 7.93 (s, 1H, N-CH=N). Yield: 34%; purity >96%.

**4.4.18. *n*-Propyl amide of *N*-methanesulfonyl-(2-amino-6-chloropureryl)-L-Ala (15).** HPLC:  $R_t$  = 13.7 min. MS (API-ES):  $m/z$  374 =  $M^+$ .  $^1H$  NMR (300 MHz, DMSO- $d_6$ ): 0.89 (t, 3H,  $J$  = 7.5 Hz,  $CH_3-CH_2-CH_2$ ), 1.40 (m, 2H,  $CH_3-CH_2-CH_2$ ), 1.58 (m, 2H,  $CH_3-CH_2-CH_2$ ), 2.32 (s, 3H,  $CH_3-SO_2$ ), 3.00 (m, 2H,  $CH-CH_2$ ), 3.84 (m, 1H,  $CH_\alpha$ ), 6.93 (m, 1H,  $NH_\alpha$ ), 7.87 (s, 1H, N-CH=N). Yield: 38%; purity >95%.

**4.4.19. Allyl amide of *N*-*p*-toluenesulfonyl-(2-amino-6-chloropureryl)-L-Ala (16).** HPLC:  $R_t$  = 13.7 min. MS (API-ES):  $m/z$  448 =  $M^+$ .  $^1H$  NMR (300 MHz, DMSO- $d_6$ ): 1.28 (m, 2H,  $CH_2=CH-CH_2$ ), 2.30 (s, 3H,  $CH_3-C_6H_4$ ), 3.47 (d, 2H,  $J$  = 5.9 Hz,  $CH_2$  ala), 5.03 (m, 1H,  $CH_\alpha$ ), 5.34 (d, 2H,  $J$  = 11.3 Hz,  $CH_2=CH$ ), 5.87 (m, 1H,  $CH_2=CH$ ), 7.12 (d, 2H,  $J$  = 7.9 Hz,  $H_{arom}$   $H_2$ ,  $H_6$ ), 7.48 (d, 2H,  $J$  = 8.0 Hz,  $H_{arom}$   $H_3$ ,  $H_5$ ), 7.99 (s, 1H, N-CH=N). Yield: 23%; purity, 95%.

**4.4.20. *n*-Propyl amide of *N*-*p*-toluenesulfonyl-(2-amino-6-chloropureryl)-L-Ala (17).** HPLC:  $R_t$  = 14.0 min. MS (API-ES):  $m/z$  450 =  $M^+$ .  $^1H$  NMR (300 MHz, DMSO- $d_6$ ): 0.92 (t, 3H,  $J$  = 7.5 Hz,  $CH_3-CH_2-CH_2$ ), 1.54 (m, 2H,  $CH_3-CH_2-CH_2$ ), 2.30 (s, 3H,  $CH_3-C_6H_4$ ), 2.75 (t, 2H,  $J$  = 7.5 Hz,  $CH_3-CH_2-CH_2$ ), 3.00 (m, 2H,  $CH_2$  ala), 7.12 (d, 2H,  $J$  = 7.8 Hz,  $H_{arom}$   $H_2$ ,  $H_6$ ), 7.48 (d, 2H,  $J$  = 7.9 Hz,  $H_{arom}$   $H_3$ ,  $H_5$ ), 7.68 (m, 3H, N-CH=N +  $NH_2$ (2-amino-6-chloropureryl)). Yield: 25%; purity, >96%.

**4.4.21. Analysis of synthesized molecules by mass spectrometry and NMR.** Analysis of aliquots was first performed on a LC/MS system (Agilent Technologies, model HP 1100 LC-MSD) with an atmospheric pressure electrospray ionization (API-ES) and a quadrupole mass spectrometer detector (MSD).<sup>48</sup> Briefly, the separation was done using a C5 reversed-phase column 0.46  $\times$  25 cm (Phenomenex, Torrance, CA, USA) at room temperature. The flow rate was 0.5 mL/min and the injection volume was 10  $\mu$ L. A linear gradient from a 10:90 to 100:0 ACN–water (with 0.1% of TFA) was used over 45 min. Mass spectrometry detection was

performed with the ESI set at Vcap = 4500 V, nebulizing gas pressure = 35 psi, drying gas flow rate = 13 L/min, drying gas temperature = 350 °C with the quadrupole scanning from 50 to 500 *m/z* every 1.03 s with a step size of 0.15 amu. The <sup>1</sup>H NMR experiments were done on a Bruker AC-F-300 MHz spectrometer using standard software. All measurements were made at 25 °C on a 5 mg sample dissolved in 0.6 mL DMSO-*d*<sub>6</sub>. The residual proton resonance of DMSO was used as an internal reference at 2.5 ppm for <sup>1</sup>H NMR spectra.

#### 4.5. Screening assay for FtsZ inhibitors

A spectrophotometric coupled enzymatic assay was developed to measure the FtsZ activity. The GTPase enzymatic reaction was quantified by monitoring the oxidation of NADH as a decrease in absorbance at 340 nm. FtsZ hydrolyzed GTP into GDP and inorganic phosphate. The GDP product is used as substrate with phosphoenol pyruvate (PEP) by the pyruvate kinase (PK) enzyme to give GTP and pyruvic acid as products. The pyruvic acid is then used as substrate with NADH + H<sup>+</sup> by the D(-)-lactate dehydrogenase (LDH) enzyme giving lactate and NAD<sup>+</sup>. The NADH + H<sup>+</sup> molecule could be detected at 340 nm but the final NAD<sup>+</sup> product gave no absorbance. The decrease in NADH + H<sup>+</sup> absorbance at 340 nm follows proportionally the FtsZ GTPase enzymatic activity (Fig. 5). This coupled enzymatic assay was optimized for specificity and for several parameters including reaction buffer, FtsZ, GTP, DTT, and DMSO. The assay contained 50 mM Bis-Tris Propane (pH 7.4), 3.5 μM of purified FtsZ, 5 mM GTP, 5 mM MgCl<sub>2</sub>, 2.5 mM DTT, 2 mM of phosphoenolpyruvate, 1.4 U of PK enzyme (Roche Diagnostics, Québec, Canada, EC: 2.1.7.40, 200 U/mg), 380 μM NADH, 2.1 U of LDH enzyme from *Lactobacillus leichmannii* (Roche Diagnostics, EC: 1.1.1.28, 300 U/mg), and 25% DMSO (Laboratoire MAT). The reaction was performed in a 100 μL volume using a Submicro Cell (Varian, Mississauga, Ontario, Canada). The optical density was monitored at 340 nm for a period of 15 min at room temperature with a Cary spectrophotometer (Varian). The FtsZ enzyme kinetics were determined from the linear portion of the curve using the least-squares calculation as described.<sup>51</sup> A negative control was performed without the FtsZ enzyme and a positive control was done using 0.5 mM GDP and without FtsZ.

#### 4.6. Inhibition assays of FtsZ and IC<sub>50</sub> determination

Each synthesized compound was dissolved in 100% DMSO at 0.1 g/L, the pH was adjusted to 7, and the buffered solution was kept at -20 °C. Inhibition of the FtsZ GTPase activity was determined using various concentrations of each GAL compound. The final DMSO concentration was adjusted to 25%. Reaction mixtures without FtsZ were incubated at 37 °C for 10 min and the FtsZ enzyme was added. The velocity of FtsZ GTPase activity was determined with each compound at various concentrations as described in Section 4.5. The percentage of GTPase residual activity was ob-

tained by comparing the enzyme velocity from each compound concentration with the velocity obtained with the wild-type FtsZ reaction. The compound concentrations required to inhibit 50% of the FtsZ GTPase activity (IC<sub>50</sub>) were obtained by plotting the percentage of residual GTPase activity.<sup>25</sup> As controls, concentrations of each compound leading to inhibition of GTPase activity were analyzed using the coupled enzymatic assay. The inhibition of enzymes in the coupled assay was evaluated by using 0.5 mM GDP without FtsZ. The velocities of the PK and LDH enzymes were determined for each compound and similar values were obtained as for the wild-type enzyme.

#### 4.7. Agar diffusion assay

Cultures of *E. coli* ATCC 25922 and *S. aureus* ATCC 25923 were grown in 10 mL of Mueller Hinton broth (MHB, Becton Dickinson Microbiology Systems, Sparks, Maryland, USA) overnight at 37 °C. The bacterial cultures were diluted in MHB to obtain a McFarland standard turbidity of 0.5. Agar plates were prepared by pouring 100 mL of Mueller Hinton Agar (Becton-Dickinson Microbiology Systems) into 150 mm Petri dishes. Plates were dried for 30 min at 37 °C and wells were made in the agar with a sterile Pasteur pipette. Sterile cotton tip applicators were used to uniformly inoculate the surface of agar plates with the bacterial cultures. As control, 100 μL DMSO and 100 μL of a 20 g/L kanamycin solution were added to wells. Each GAL compound was diluted in DMSO to reach a 20 g/L concentration and 100 μL of each solution (2 mg) was added to wells. Plates were incubated at 37 °C overnight without being inverted.

#### Acknowledgments

This work was supported by a FQRNT team grant to Roger C. Levesque. Catherine Paradis-Bleau obtained a studentship from Le Fonds de la Recherche en Santé du Québec and Mélanie Beaumont obtained a CREF-SIP studentship. R. C. Levesque is a FRSQ scholar of exceptional merit.

#### References and notes

1. Levy, S. B.; Marshall, B. *Nat. Med.* **2004**, *10*, S122.
2. Margolin, W. *Nat. Rev. Mol. Cell. Biol.* **2005**, *6*, 862.
3. Projan, S. J. *Curr. Opin. Pharmacol.* **2002**, *2*, 513.
4. van den Ent, F.; Amos, L.; Lowe, J. *Curr. Opin. Microbiol.* **2001**, *4*, 634.
5. Lutkenhaus, J.; Addinall, S. G. *Annu. Rev. Biochem.* **1997**, *66*, 93.
6. de Boer, P.; Crossley, R.; Rothfield, L. *Nature* **1992**, *359*, 254.
7. Errington, J.; Daniel, R. A.; Scheffers, D. J. *Microbiol. Mol. Biol. Rev.* **2003**, *67*, 52.
8. Cordell, S. C.; Robinson, E. J.; Lowe, J. *Proc. Natl. Acad. Sci. U.S.A.* **2003**, *100*, 7889.
9. Pierce, G. E. J. *Ind. Microbiol. Biotechnol.* **2005**, *32*, 309.
10. Hoiby, N. J. *Cyst. Fibros.* **2002**, *1*, 249.
11. Plunkett, M. J.; Ellman, J. A. *Sci. Am.* **1997**, *276*, 68.

12. Balkenhahl, F.; Bussche-Hünnefeld, C.; Lansky, A.; Zechel, C. *Angew. Chem., Int. Ed. Engl.* **1996**, *35*, 2288.
13. Arnold, L. D.; Kalantar, T. H.; John, C. *J. Am. Chem. Soc.* **1985**, *107*, 7105.
14. Ciapetti, P.; Soccilini, F.; Taddei, M. *Tetrahedron* **1997**, *53*, 1167.
15. Sliedregta, K. M.; Schoutenb, A.; Kroonb, J.; Rob, M. J. *Tetrahedron Lett.* **1996**, *37*, 4237.
16. Bodanszky, M. *Peptide Chemistry: A Practical Textbook*; Springer Verlag: Berlin, New York, 1988, p 58.
17. Breithaupt, H. *Nat. Biotechnol.* **1999**, *17*, 1165.
18. Diaz, J. F.; Kralicek, A.; Mingorance, J.; Palacios, J. M.; Vicente, M., et al. *J. Biol. Chem.* **2001**, *276*, 17307.
19. Marrington, R.; Small, E.; Rodger, A.; Dafforn, T. R.; Addinall, S. G. *J. Biol. Chem.* **2004**, *279*, 48821.
20. Lewis, I. *Tetrahedron Lett.* **1993**, *34*, 5697.
21. Pansare, S. V.; Arnold, L. D.; Vederas, J. C. *Org. Syn.* **1993**, *70*, 10.
22. Pansare, S. V.; Huyer, G.; Arnold, L. D.; Vederas, J. C. *Org. Syn.* **1993**, *70*, 1.
23. De Grado, W. F.; Kaiser, E. T. *J. Org. Chem.* **1980**, *45*, 1295.
24. De Grado, W. F.; Kaiser, E. T. *J. Org. Chem.* **1982**, *47*, 3258.
25. Paradis-Bleau, C.; Sanschagrín, F.; Levesque, R. C. *J. Antimicrob. Chemother.* **2004**, *54*, 278.
26. Sosson, T. M., Jr.; Brigham-Burke, M. R.; Hensley, P.; Pearce, K. H., Jr. *Biochemistry* **1999**, *38*, 14843.
27. Bramhill, D.; Thompson, C. M. *Proc. Natl. Acad. Sci. U.S.A.* **1994**, *91*, 5813.
28. Mukherjee, A.; Cao, C.; Lutkenhaus, J. *Proc. Natl. Acad. Sci. U.S.A.* **1998**, *95*, 2885.
29. Thompson, L. A.; Ellman, J. A. *Chem. Rev.* **1996**, *96*, 555.
30. Hughes, D. *Nat. Rev. Genet.* **2003**, *4*, 432.
31. Nefzi, A.; Dooley, C.; Ostresh, J. M.; Houghten, R. A. *Bioorg. Med. Chem. Lett.* **1998**, *8*, 2273.
32. Nogales, E.; Downing, K. H.; Amos, L. A.; Lowe, J. *Nat. Struct. Biol.* **1998**, *5*, 451.
33. Carballido-Lopez, R.; Errington, J. *Trends Cell. Biol.* **2003**, *13*, 577.
34. Leung, A. K.; Lucile White, E.; Ross, L. J.; Reynolds, R. C.; DeVito, J. A., et al. *J. Mol. Biol.* **2004**, *342*, 953.
35. Yu, X. C.; Margolin, W.; Gonzalez-Garay, M. L.; Cabral, F. *J. Cell. Sci.* **1999**, *112*, 2301.
36. White, E. L.; Suling, W. J.; Ross, L. J.; Seitz, L. E.; Reynolds, R. C. *J. Antimicrob. Chemother.* **2002**, *50*, 111.
37. Stokes, N. R.; Sievers, J.; Barker, S.; Bennett, J. M.; Brown, D. R., et al. *J. Biol. Chem.* **2005**, *280*, 39709.
38. Jennings, L. D.; Foreman, K. W.; Rush, T. S., 3rd; Tsao, D. H.; Mosyak, L., et al. *Bioorg. Med. Chem.* **2004**, *12*, 5115.
39. Reynolds, R. C.; Srivastava, S.; Ross, L. J.; Suling, W. J.; White, E. L. *Bioorg. Med. Chem. Lett.* **2004**, *14*, 3161.
40. Urgaonkar, S.; La Pierre, H. S.; Meir, I.; Lund, H.; RayChaudhuri, D., et al. *Org. Lett.* **2005**, *7*, 5609.
41. Wang, J.; Galgocsi, A.; Kodali, S.; Herath, K. B.; Jayasuriya, H., et al. *J. Biol. Chem.* **2003**, *278*, 44424.
42. RayChaudhuri, D.; Park, J. T. *Nature* **1992**, *359*, 251.
43. Margalit, D. N.; Romberg, L.; Mets, R. B.; Hebert, A. M.; Mitchison, T. J., et al. *Proc. Natl. Acad. Sci. U.S.A.* **2004**, *101*, 11821.
44. Lappchen, T.; Hartog, A. F.; Pinas, V. A.; Koomen, G. J.; den Blaauwen, T. *Biochemistry* **2005**, *44*, 7879.
45. Paradis-Bleau, C.; Sanschagrín, F.; Levesque, R. C. *Protein Eng. Des. Sel.* **2005**, *18*, 85.
46. Zhulanova, E.; Mikulik, K. *Biochem. Biophys. Res. Commun.* **1998**, *249*, 556.
47. Feucht, A.; Lucet, I.; Yudkin, M. D.; Errington, J. *Mol. Microbiol.* **2001**, *40*, 115.
48. Zoeiby, A. E.; Beaumont, M.; Dubuc, E.; Sanschagrín, F.; Voyer, N., et al. *Bioorg. Med. Chem.* **2003**, *11*, 1583.
49. Stewart, J. M.; Young, J. D. *In Solid Phase Synthesis*; Pierce Chemical Company: Rockford, Illinois, 1984, p 105.
50. Voyer, N.; Lavoie, A.; Pinette, M.; Bernier, J. *Tetrahedron Lett.* **1994**, *35*, 355.
51. Savoie, A.; Sanschagrín, F.; Palzkill, T.; Voyer, N.; Levesque, R. C. *Protein Eng.* **2000**, *13*, 267.